JKAU: Eng. Sci., **Vol. 34 No. 2**, pp: 53–51 (2024A.D.)
DOI:10.4197/Eng.34-2.4

Modeling and optimizing electro Fenton process for silica removal to prevent RO membrane fouling in brackish water desalination.

Ahmad Yahya, Fathi Djouider

King Abdulaziz University, Dept Nuclear Engineering, Jeddah 80204, Saudi Arabia

atahar@kau.edu.sa

Abstract: Due to high silica concentrations, silica scaling of reverse osmosis (RO) membranes in brackish water desalination poses serious issues with cost-effectiveness of desalination processes. The advanced Fenton process (AFP) is one of the most effective water treatment processes. Coagulation of silica with ferric hydroxide and flocculation are the main processes used to remove silica. This process depends on several operating parameters such as hydrogen peroxide and zero-valent metal iron Fe^0 dosage, initial and equilibrium pH. In this study, we examined the use of Artificial Neural Networks (ANNs) to optimize those parameters using an experimental dataset. For a removal of 71.3%, the optimum operating parameters were: initial pH 2, equilibrium pH 8, iron dosage 15 g/L and hydrogen peroxide 18 mM. This study demonstrates the economic feasibility of the environmentally friendly Fenton process, achieving up to 71.2% silica removal at a total cost of \$2.09 m^{-3} for a typical 1,000 m^3/day desilication unit.

Keywords: Silica removal, Water desalination, Artificial intelligence, Neural networks

1. Introduction

Water resources in most arid countries come from the desalination of seawater and brackish underground water from deep non-renewable sedimentary aquifers [1]. Before use, these waters must be desalinated. The most widely used treatment method is reverse osmosis (RO) using semi-permeable membranes to trap dissolved salts [2, 3].

Silica, orthosilicic acid, $Si(OH)_4$, originates from the chemical weathering of silica-containing minerals such as quartz and feldspar [4]. Its concentration in brackish water is high. During RO desalination, it does not diffuse through the membrane, clogging the latter. This will cause its refractory deposit on the RO membrane during desalination [5], posing a major challenge to the cost-effectiveness of freshwater production. However, desilication is relatively expensive, accounting for up to 80% of a water treatment plant's operational cost [6].

There are several different treatment methods for removing silica, including coagulation with metal hydroxides [7, 8], flocculation [9], nanofiltration [10], and utilizing the use of anti-scaling agents [11]. Throughout the last few decades, advanced oxidation processes have demonstrated their great effectiveness in water treatment procedures [12-16]. One of the main advanced oxidation treatment methods is the Fenton process, which involves the generation of hydroxyl radicals ($OH^{\bullet}$) [17].

The efficacy of the Fenton process for the degradation of organic compounds decreases at both high and low pH values. Furthermore, the Fenton reaction system is subject to various competitive reactions that can hinder its effectiveness. In the case of Fenton oxidation, the rate of reaction is influenced by the dosage of iron, while the extent of mineralization is directly proportional to the concentration of the oxidant. The main disadvantages of the Fenton process are the relatively high cost of H_2O_2 and the large amount of ferric sludge produced in the neutralization step of the treated solution before disposal.

This study aims to use artificial intelligence (AI) to optimize the parameters involved in the reaction to achieve the highest silica removal possible. This approach is becoming common in many research fields [21-23] and gained interest in water treatment research in recent years [24-27].

The AI model will be based on artificial neural networks (ANNs) to optimize the parameters. It can also help us minimize the cost of the treatment operation by showing if the use of H_2O_2 can be reduced while optimizing the other parameters without compromising water treatment quality.

ANNs can be used for multiple tasks, including classification, regression, and prediction. In the case of prediction, ANNs can be trained on a dataset of historical data, and then used to make predictions about future data.

To use an ANN for prediction, the model is first trained on a labeled dataset with a process known as backpropagation. During training, the model adjusts its weights and biases to minimize the difference between its predicted and actual output in the training dataset. Once the model is trained, it can be used to make predictions on new, unlabeled data.

The model developed in this work can also help us minimize the cost of the treatment operation by showing if the use of H_2O_2 can be reduced while optimizing the other parameters without compromising water treatment quality.

2. Materials and methods

2.1 Removal mechanisms of the Fenton process.

Under acidic conditions, the advanced Fenton process uses the oxidation of metallic iron

and hydrogen peroxide, H_2O_2, to generate ferric ions to generate the hydroxyl free radical $OH^{\bullet}$ [18,19]:

$$Fe + 2\,H^{+} \rightarrow Fe^{2+} + H_2$$

$$Fe^{2+} + H_2O_2 \rightarrow Fe^{3+} + OH^{\bullet} + OH^{-}$$

After its hydrolysis

$$Fe^{3+} + 3\,H_2O \rightarrow 3\,H^{+} + Fe(OH)_3$$

ferric hydroxide is known to coagulate on the silica by weak van der Waals attraction to form a silico-ferric hydro-complex [20], which is then removed from the bulk by settling or filtration:

$$Fe(OH)_3 + Si(OH)_4 \rightarrow [SiO_2 - Fe(OH)_3] + 2H_2O$$

Figure 1 presents a simplified representation of a potential treatment pathway for brackish water desalination utilizing the Fenton process. Influent water first encounters a potential pH adjustment stage. By altering the pH (often to a slightly acidic range), silica solubility can be

manipulated, promoting its precipitation or improving its interaction with products of the Fenton reaction. Hydrogen peroxide (H_2O_2) is then introduced, and iron (Fe) catalysts trigger the reaction, generating hydroxyl radicals (OH•) degrading organic matter and contaminants. These highly reactive radicals, along with the potentially adjusted pH, can promote the precipitation or coagulation of dissolved silica from the brackish water. Following this pretreatment, further purification steps like filtration or reverse osmosis (RO) remove the targeted salts (ions) and any remaining silica particulates, ensuring the desalinated water meets specific quality requirements.

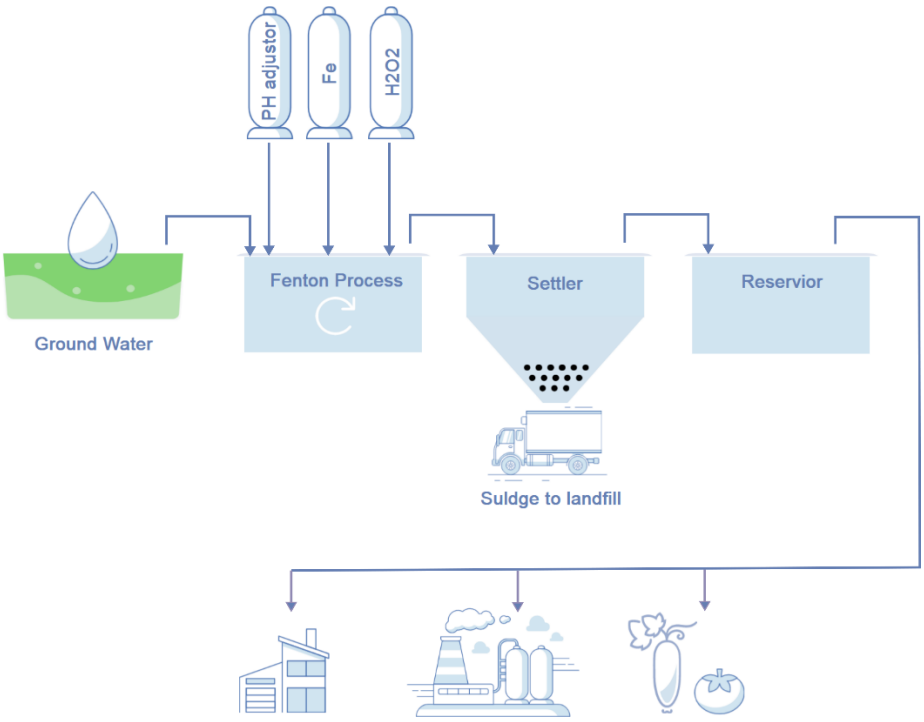

Figure 1: Cycle of the Fenton brackish underground water desilication and the use of permeate water.

2.2 Artificial neural networks (ANNs)

ANNs are a machine learning model inspired by the structure and function of the human brain. ANNs consist of interconnected nodes, or neurons, organized into layers. Information flows through the network from the input layer, through one or more hidden layers, and finally to the output layer. Each neuron in the network receives inputs from other neurons and processes them to produce an output signal passed on to the next layer. The architecture of an ANN can vary widely depending on the specific task and the data used. However, some common types of layers are often used in ANNs:

1. Input layer: This is the first layer of the network and consists of neurons that receive input data.
2. Hidden layer: This layer processes the input data and performs computations.
3. Output layer: This is the final layer of the network and produces the predicted output based on the

computations performed by the hidden layer.

Other important terms of the ANN are the weights, bias, and activation function.

Weights are the parameters that determine the strength of the connections between neurons. During training, the ANN adjusts these weights to optimize the model performance. A bias is an additional parameter in an ANN that allows the network to shift the output of a neuron. Without a bias, the output of a neuron would always be zero when the input is zero. By adding a bias, the neuron can output a non-zero value even when the input is zero. Like weights, biases are adjusted during training to optimize performance. The transfer function, also known as the activation function, is a mathematical function applied to the output of each neuron in an ANN. The activation function determines whether the neuron should "fire" based on its input. Commonly used activation functions include the sigmoid function, the rectified linear unit (ReLU) function, and the hyperbolic tangent function. The choice of transfer function depends on the specific task and the properties of the data being used.

2.3 Dataset

The dataset used was obtained from the study by Djouider and Aljohani [20]. The study used the advanced Fenton process for the treatment of silica in underground raw water samples from the Buwaib water desalination plant near the capital city of Riyadh, Saudi Arabia. The input parameters were the initial pH, H_2O_2 concentration, Fe concentration, equilibrium pH, and the processing time in hours. The output measured was the silica removal percentage. There were 57 dataset entries for our model. The dataset is provided on GitHub [28].

2.4 ANN architecture

Our investigation employed the MATLAB R2020a platform to generate a customized ANN model. Specifically, we utilized the "nftool" app integrated into MATLAB to construct a type of ANN called a feed-forward network with one hidden layer (shallow network). The ANN model was established with a few neurons in the input, output, and hidden layer. The ANN architecture comprised an input layer with neurons equivalent to the number of independent input variables (5), an output layer with neurons corresponding to the single output (silica removal), and a single hidden layer.

The output of the ANN model can be described by the following function:

$$y = f_2(\sum_m \widetilde{w}_m(f1\sum_n(w_{nm}I_n + b_m)) + b) \quad (1)$$

Where y, f, w, I, and b are the output, activation function, weight, input, and bias value, respectively. The letters n and m represent the order of the inputs, weights, and bias values, as shown in Figure 2. Table 1 summarizes the features of the ANN models that were tested and the percentage of data allocated for training, validation and testing.

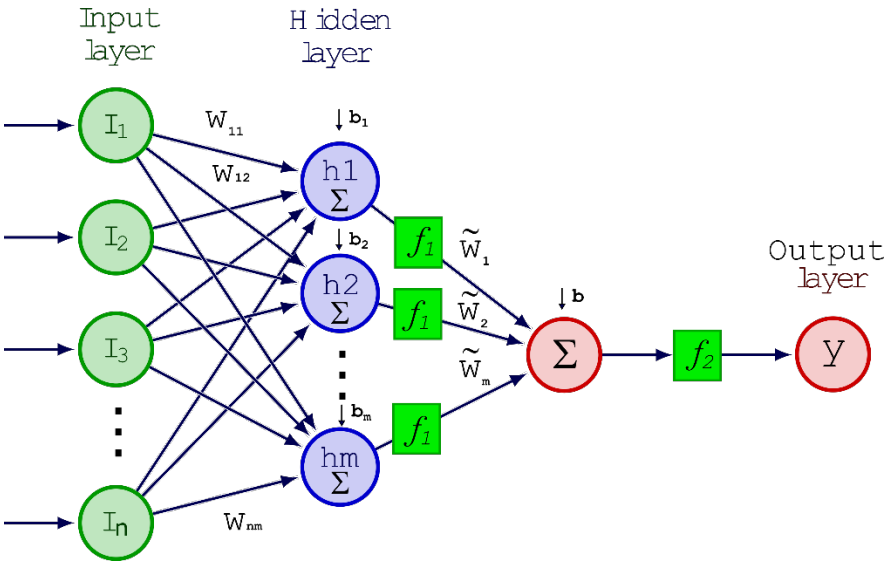

Figure 2: ANN model architecture.

Table 1: ANN model parameters and training settings.

Parameter/Setting	Symbol	Value
Input layer size	*I*	5
Output layer size	*Y*	1
Hidden layer size	*H*	2 to 4
Activation function for the hidden layer	f_1	Sigmoid
Activation function for the output layer	f_2	Linear
Training function	--	Levenberg-Marquardt, Bayesian regularization, and scaled conjugate gradient function
Performance measuring function	--	MSE
Training dataset percentage	--	70%
Validation dataset percentage	--	15%
Test dataset percentage	--	15%

2.5 Network training

In this study, training a shallow neural network involves finding the weights and biases that produce computed outputs close to the observed target values for the training data set. The 'train' function was used to develop models using batch training, where all input vectors are presented to the network in one epoch (run) of training. The weights are updated after calculating the mean square error (MSE) at the end of the run. Available data was divided into three sets: training, validation, and testing, with 70%, 15%, and 15% of the data given to each set respectively. The best-performing algorithm was selected based on trial and error by testing three backpropagation algorithms (training algorithms) for several runs. The model performance was evaluated using the R^2 value and the MSE.

$$R^2 = \frac{\sum_i(\hat{y}_i-\bar{y})^2}{\sum_i(y_i-\bar{y})^2} \quad (2)$$

$$MSE = \frac{1}{n}\sum_{i=1}^{n}(y_i - \hat{y})^2 \quad (3)$$

Where y_i, $\hat{y}_i$, and $\bar{y}$ are the experimental value, the predicted value, and the mean value respectively.

3. Results and discussion

3.1 Model development results and regression analysis

Nine feed-forward models were constructed by varying the training function and the number of nodes in the hidden layer. The training functions were the Levenberg-Marquardt function, the Bayesian regularization function, and the scaled conjugate gradient function. The nodes in the hidden layer ranged from 2 to 4. The first and second activation functions (f_1 and f_2) remained fixed as a sigmoid and linear function, respectively.

Table 2 shows the maximum performance for the ANN models by varying the training functions and the number of nodes in the hidden layer.

From trial and error over several runs for each case, the best model was found to have an R^2-value of 99.12% using the Levenberg-Marquardt function with 3 nodes in the hidden layer.

Figure 3 shows the regression analysis for the training, validation, test, and all three combined. The plots illustrate an excellent fit of the actual silica removal results with the prediction of the model in all three sets with 99% and above.

Table 2: Models parameters and performance metrics.

Model	Training function	Hidden layer activation function	Output layer activation function	Hidden layer nodes	MSE $_{Test}$	R $_{Test}$
1	Levenberg-Marquardt	Sigmoid	Linear	2	43.114	0.967
2				**3**	**16.197**	**0.991**
3				4	18.427	0.990
4	Bayesian Regularization			2	41.838	0.980
5				3	41.062	0.985
6				4	45.606	0.981
7	Scaled Conjugate Gradient (SCG)			2	59.041	0.948
8				3	75.446	0.959
9				4	19.966	0.989

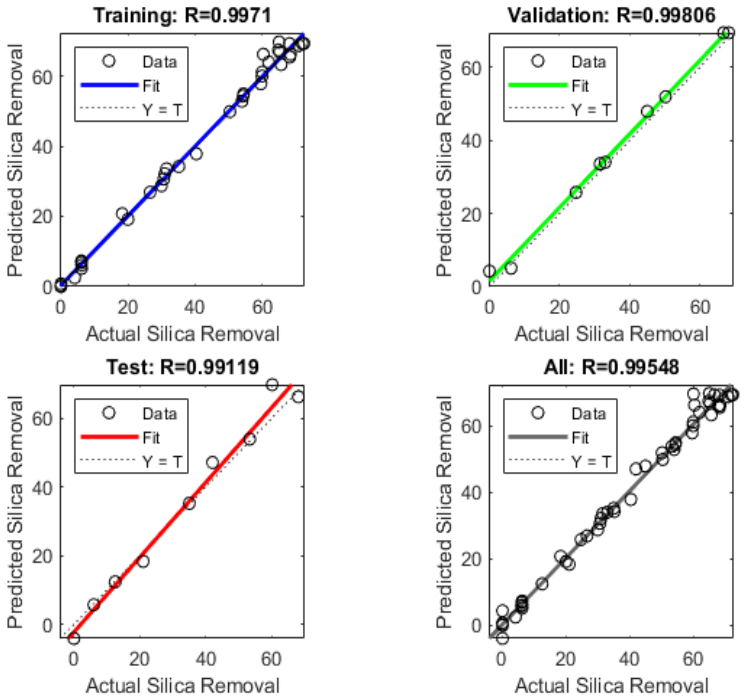

Figure 3: Regression analysis for the training, validation, and test sets.

Figure 4 shows the performance of the training, validation and test sets. The three curves represent the model's performance on the training data (blue), validation data (green), and test data (red). Notably, the best validation performance is achieved at epoch 18. Although the validation curve (green) doesn't exhibit a clear plateau before this point, all three curves converge around epoch 18, suggesting the model has learned the underlying trend and generalizes reasonably well to unseen data. The small and consistent gaps between the curves further indicate that the model's performance on the training data translates effectively to unseen data on the validation and test sets. The test set performance (red) is slightly lower than the validation performance (green), as expected for unseen data. This convergence of performance curves and the small gaps between them provide evidence for the model's successful generalization.

3.2 Absolute difference and ANOVA results

Calculating the absolute difference between the actual and predicted removal results showed that the highest variance in the prediction was 9.6 away from the actual removal percentage. Most prediction results (51 out of 57) were only 0-3.2% more or less than the actual results (Figure 5). The result of the ANOVA test is demonstrated in Table S1. The F value was 0.006, indicating with a 95% level of confidence that there is no significant difference between the actual and predicted values. The results suggest that the model can predict the outcome of the Fenton process for removing silica with high accuracy. The algorithm and weights can be found on GitHub [23] for ease of access for future users.

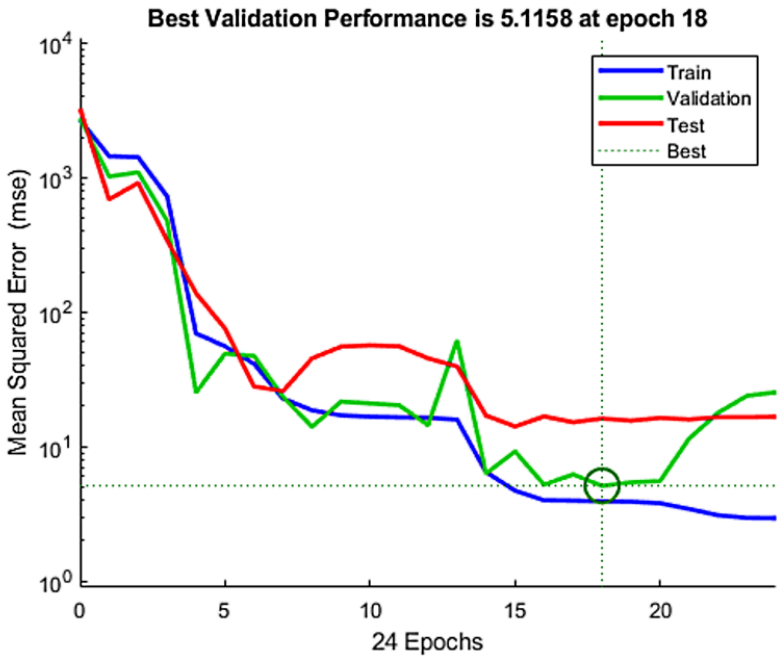

Figure 4: Best Validation performance showing MSE results of the training, validation, and test sets.

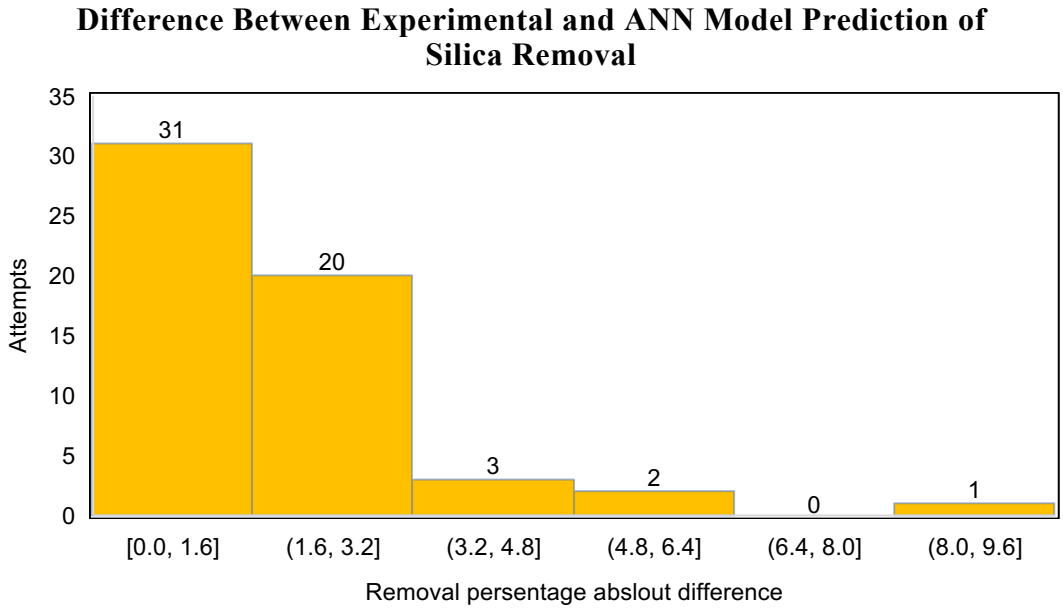

Figure 5: Absolute difference between actual and predicted results.

3.3 Data extrapolation

The model was used to extrapolate silica removal results for a range of values for each parameter; for more details refer to Table S2. The model predicted 11,700 results in total.

The maximum silica removal from the experimental process was 72.5%. This result was achieved using the following values, initial pH: 2, equilibrium pH: 8, H_2O_2: 15 mM, Fe: 8 g/L, and time: 3.5 hr. As the original experiments tested the removal for up to 3.5 hours, it was interesting to know if increasing the time would significantly increase the process output. Figure 6 shows how the model predicted the results with increasing time. There is no significant difference in removal in increasing the Fenton process

time, as it will delay water production and reduce profits for a water treatment plant.

Next, the varying concentrations of H_2O_2 and Fe were studied while the remaining parameters remained constant as follows, initial pH: 2, equilibrium pH: 8, and time: 5 hr. Figure 7 shows how the results were predicted. Most of the results were comparable, ranging from around 69% to just above 71%. Only when the concentration of H_2O_2 was about 18 to 20 mM and the Fe was around 8 to 10 g/L did the removal start to do drop until it reached 52%.

From these results, one can conclude that even if the H_2O_2 and Fe concentration and the treatment time increased, the removal of silica will not increase, and so it is recommended not to add any extra expenses to the process by adding more volumes of these materials or time, as it will not increase its efficiency.

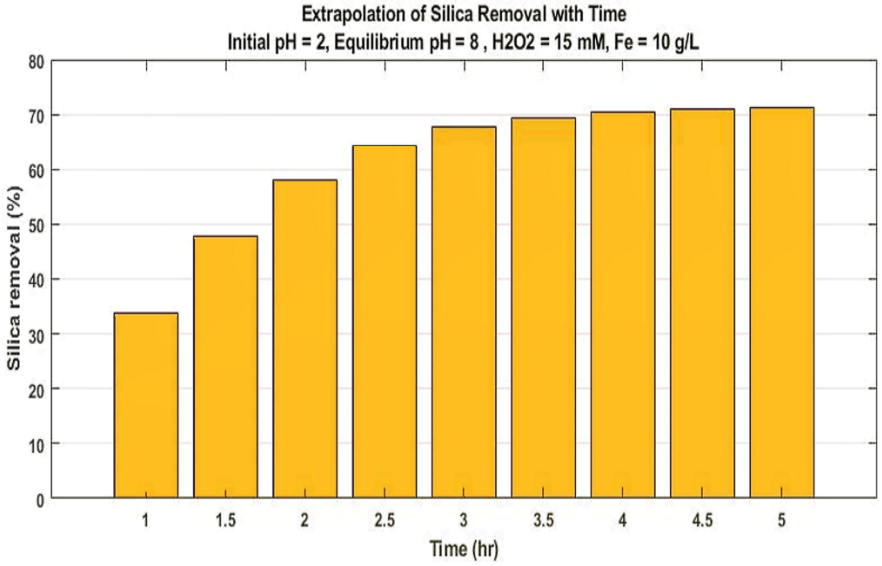

Figure 6: Extrapolation of silica removal with time using the same parameters that gave the optimum result in the actual experiment. Not much improvement is expected with increasing time.

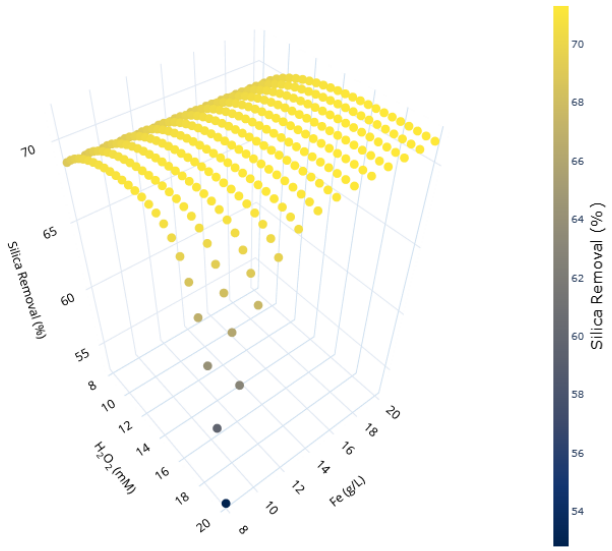

Figure 7: Silica removal with varying Fe and H_2O_2 quantities, initial pH: 2, equilibrium pH: 8, and time: 5 hr.

3.4 Cost analysis

The process cost is a major concern for water treatment stockholders. Pretreatment chemicals, labor, and maintenance costs were considered in calculating the overall treatment cost. If municipal stabilization ponds are considered, the discharge of sludge cost is relatively low compared to other disposal systems. The operational cost, in terms of the price of silica removal per cubic meter of raw water treated ($ m^{-3}), can be calculated as:

$$Operation\ cost = a \times CC + LC + MC \quad (4)$$

a: cost of chemical ($/kg), CC is the chemical consumption (in $kg.m^{-3}$), LC is the labor cost, and MC is the maintenance cost.

The cost was calculated based on the wholesale prices in the Middle East region at the time of writing this article. The lowest cost was $2.58/$m^3$. Table 3 shows the quantities needed for H_2O_2 and Fe.

Table 3: Chemical values for best removal results and lowest cost for Silica removal.

Initial pH	**Equilibrium pH**	**H_2O_2 mM**	**Fe g/L**	**Time Hr.**	**Removal $_{Prediction}$ (%)**	**Cost (U.S. Dollars)/ m^3**
2	8	18	15	5	71.29	2.58
2	8	16	11	5	71.21	2.09

Assuming treating 1,000 m^3/day for 365 days, a treatment station will save $178,850 annually if it spends $2.09/$m^3$ compared to $2.58/$m^3$, without compromising removal efficiency.

Labor cost: If three workers are to run this unit, with an average monthly salary of $1500 each, the labor cost would be $54,000/ year. Other costs: Other maintenance costs (spare parts, pumps…etc.) are included in the capital cost and would be $0.5/$m^3$ [29].

For a typical small desilication unit treating 1,000 m^3/day, the total annual cost of spending $8.2/$m^3$ on chemicals will be:

$54,000 + $(2.09 x 1000 x365) + $(0.5 x 1000 x 365) ≈ $999,350/year.

4. Conclusion

An Artificial Neural Network model was developed to optimize the parameters for silica removal. The dataset consisted of 57 entries, with input parameters including initial pH, H_2O_2 concentration, Fe concentration, equilibrium pH, and processing time in hours, while the output measured was the silica removal percentage.

The ANN architecture employed a feed-forward network with one hidden layer, comprising an input layer with 5 neurons, an output layer, and a few neurons in the hidden layer. The optimized operating parameters for a silica removal of 71.3% were determined to be initial pH 2, equilibrium pH 8, iron dosage of 15 g/L, and hydrogen peroxide concentration of 18 mM.

The model's predictions indicated that increasing the processing time did not significantly affect the silica removal, suggesting that prolonging the Fenton process could lead to decreased water production and reduced profits for a water treatment plant. Furthermore, varying concentrations of H_2O_2 and Fe while keeping other parameters constant showed

that the silica removal did not increase significantly with higher concentrations of these substances.

The model's findings are valuable as they provide insights into optimizing the Fenton process parameters for efficient silica removal, potentially reducing costs associated with water treatment operations without compromising water quality.

5. Limitations.

The dataset used was small and more data is needed to generalize the model to a wider range of values.

6. Future Work.

In the future, the predictions will be tested with actual experiments to confirm the model's reliability.

7. Funding.

This research received no external funding.

8. References

[1] **McDonald, R.I., Douglas, I., Revenga, C., Hale, R., Grimm, N., Grönwall, J.** and **Fekete, B.,** Global Urban Growth and the Geography of Water Availability, Quality, and Delivery, *Ambio,* 40, 437-446, (2011).

[2] **Liu, X., Shanbhag, S., Bartholomew, T.V., Whitacre, J.F.** and **Mauter, M.S.,** Cost Comparison of Capacitive Deionization and Reverse Osmosis for Brackish Water Desalination, *ACS ES&T Eng.,* 1, 261-273, (2021).

[3] **Subramani, A.** and **Jacangelo, J.G.,** Treatment Technologies for Reverse Osmosis Concentrate Volume Minimization: A Review, *Sep. Purif. Technol.,* 122, 472-489, (2014).

[4] **Crundwell, F.K.,** On the Mechanism of the Dissolution of Quartz and Silica in Aqueous Solutions, *ACS Omega*, 2, 1116-1127, (2017).

[5] **Jiang, S., Li, Y.** and **Ladewig, B.P.,** A Review of Reverse Osmosis Membrane Fouling and Control Strategies, *Sci. Total Environ*., 595, 567-583, (2017).

[6] **Pedenau, P.** and **Dang, F.,** A New Water Treatment Scheme for Thermal Development: The SIBE Process, Proc. of the International Thermal Operations and Heavy Oil Symposium, Society of Petroleum Engineers, Calgary, Alberta, Canada, (2008).

[7] **Salvador Cob, S., Hofs, B., Maffezzoni, C., Adamus, J., Siegers, W.G., Cornelissen, E.R., Genceli Güner, F.E.** and **Witkamp, G.J.,** Silica Removal to Prevent Silica Scaling in Reverse Osmosis Membranes, *Desalination,* 344, 137-143, (2014).

[8] **Semiat, R., Sutzkover, I.** and **Hasson, D.,** Scaling of RO Membranes from Silica Supersaturated Solutions, *Desalination*, 57, 169-191, (2003).

[9] **Liu, R., Xue, T., Song, J., Wang, Y., Qi, T., Qu, J.** and **Du, A.,** Removal of Silicon in Acid Leaching and

Flocculation Processes During Zirconium Oxychloride Octahydrate Production, *Ceram. Int.,* 40, 8801-8808, (2014).

[10] **Molinari, R., Argurio, P.** and **Romeo, L.,** Studies on Interactions Between Membranes (RO and NF) and Pollutants (SiO_2, NO^{3-}, Mn^{++} and Humic Acid) in Water, *Desalination*, 138, 271-281, (2001).

[11] **Ning, R.Y., Troyer, T.L.** and **Tominello, R.S.,** Chemical Control of Colloidal Fouling of Reverse Osmosis Systems, *Desalination*, 172, 1-6, (2005).

[12] **Bergendahl, J., Hubbard, S.** and **Grasso, D.,** Pilot-Scale Fenton's Oxidation of Organic Contaminants in Groundwater Using Autochthonous Iron, *J. Hazard. Mater*., 99, 43-56, (2003).

[13] **Chidambara Raj, C.B.** and **Quen, H.L.,** Advanced Oxidation Processes for Wastewater Treatment: Optimization of UV/H2O2 Process Through a Statistical Technique, *Chem. Eng. Sci.,* 60, 5305-5311, (2005).

[14] **Xu, M., Wang, Q.** and **Hao, Y.I.,** Removal of Organic Carbon from Wastepaper Pulp Effluent by Lab-Scale Solar Photo-Fenton Process, *J. Hazard. Mater*., 148, 103-109, (2007).

[15] **Matta, R., Hanna, K.** and **Chiron, S.,** Fenton-Like Oxidation of 2,4,6-Trinitrotoluene Using Different Iron Minerals, *Sci. Total Environ*., 385, 242-251, (2007).

[16] **Lucking, F., Koser, H., Jank, M.** and **Ritter, A.,** Iron Powder and Graphite and Activated Carbon as a Catalyst for the Oxidation of 4-Chlorophenol with Hydrogen Peroxide in Aqueous Solution, *Water Res.,* 32, 2607-2614, (1998).

[17] **Guimarães, B.S., et al.,** Environmentally Friendly System for the Degradation of Multipesticide Residues in Aqueous Media by the Fenton's Reaction, *Environ. Sci. Pollut. Res.,* 21, 584-592, (2014).

[18] **Bergendahl, J.** and **Thies, T.,** Fenton's Oxidation of MTBE with Zero-Valent Iron, *Water Res.*, 38, 327-334, (2004).

[19] **Aljohani, M.S.,** Laboratory-Scale Study of the Advanced Fenton Process for Silica Removal from Brackish Underground Water in Arid Areas in Saudi Arabia, *Desalination and Water Treatment,* 65, 60-66, (2017).

[20] **Aljohani, M.S.,** Synergistic Efficiency of the Desilication of Brackish Underground Water in Saudi Arabia by Coupling γ-Radiation and Fenton Process: Membrane Scaling Prevention in Reverse Osmosis Process, *Radiation Physics and Chemistry*, 141, 245-250, (2017).

[21] **Zhang, P., et al.,** AI-Enabled Space-Air-Ground Integrated Networks: Management and Optimization, IEEE Network, (2023).

[22] **Olabi, A.G., et al.,** Application of Artificial Intelligence for Prediction, Optimization, and Control of Thermal Energy Storage Systems, *Thermal Science and Engineering Progress*, 39, Art. no. 101730, (2023).

[23] **Siva Shankar, S., et al.,** A Novel Optimization Based Deep Learning with Artificial Intelligence Approach to Detect Intrusion Attack in Network System, *Education and Information Technologies,* 29, 3859-3883, (2024).

[24] **Zhuang, X., et al.,** Multi-Objective Optimization of Reservoir Development Strategy with Hybrid Artificial Intelligence Method, *Expert Systems with*

Applications, 241, Art. no. 122707, (2024).

[25] **Saboe, D., et al.,** Real-Time Monitoring and Prediction of Water Quality Parameters and Algae Concentrations Using Microbial Potentiometric Sensor Signals and Machine Learning Tools, *Science of the Total Environment*, 764, Art. no. 142876, (2021).

[26] **Sayed, E.T., Rezk, H., Abdelkareem, M.A.** and **Olabi, A.G.,** Artificial Neural Network Based Modelling and Optimization of Microalgae Microbial Fuel Cell, *International Journal of Hydrogen Energy*, 52, 1015-1025, (2024).

[27] **Singh, V.** and **Mishra, V.,** Evaluation of the Effects of Input Variables on the Growth of Two Microalgae Classes During Wastewater Treatment, *Water Research*, 213, Art. no. 118165, (2022).

[28] **Ahmad ATY,** Ahmad ATY/Slica-ANN, GitHub, Dec. 07, (2023).

[29] **Rueda-Márquez, J.J., Levchuk, I., Manzano, M.** and **Sillanpää, M.,** Toxicity Reduction of Industrial and Municipal Wastewater by Advanced Oxidation Processes (Photo-Fenton, UVC/H_2O_2, Electro-Fenton and Galvanic Fenton): A Review, *Catalysts*, 10, 612, (2020).

نمذجة وتحسين عملية الفنتون الكهربائية لإزالة السيليكا لمنع تلوث غشاء في تحلية المياه المالحة.

احمد يحيى، فتحي جويدر

جامعة الملك عبد العزيز، قسم الهندسة النووية، جدة 80204، المملكة العربية السعودية
atahar@kau.edu.sa

ملخص: بسبب التركيزات العالية من السيليكا، فإن تقشر السيليكا في أغشية التناضح العكسي (RO) في تحلية المياه المالحة يطرح مشكلات خطيرة فيما يتعلق بفعالية تكلفة عمليات تحلية المياه. تعد عملية فنتون المتقدمة (AFP) واحدة من أكثر عمليات معالجة المياه فعالية. تخثر السيليكا مع هيدروكسيد الحديديك والتلبد هي العمليات الرئيسية المستخدمة لإزالة السيليكا. تعتمد هذه العملية على عدة عوامل تشغيل مثل بيروكسيد الهيدروجين وجرعة معدن الحديد صفر التكافؤ Fe^0، ودرجة الحموضة الأولية والتوازنية. في هذه الدراسة، قمنا بفحص استخدام الشبكات العصبية الاصطناعية (ANNs) لتحسين تلك المعلمات باستخدام مجموعة بيانات تجريبية. لإزالة 71.3%، كانت معلمات التشغيل المثلى هي: الرقم الهيدروجيني الأولي ، توازن الرقم الهيدروجيني 8، جرعة الحديد 15 جم / لتر وبيروكسيد الهيدروجين 18 ملم. توضح هذه الدراسة الجدوى الاقتصادية لعملية فنتون الصديقة للبيئة، حيث حققت إزالة ما يصل إلى 71.2% من السيليكا بتكلفة إجمالية قدرها 2.09 دولار م^3 لوحدة إزالة السيليكات النموذجية بقدرة 1000 م^3/يوم.

الكلمات المفتاحية: إزالة السيليكا، تحلية المياه، الذكاء الاصطناعي، الشبكات العصبية